NANO LETTERS

2008
Vol. 8, No. 6
1713-1718

In Spite of Recent Doubts Carrier Multiplication Does Occur in PbSe Nanocrystals

M. Tuan Trinh,[†] Arjan J. Houtepen,[*,†] Juleon M. Schins,[*,†] Tobias Hanrath,[‡] Jorge Piris,[†] Walter Knulst,[†] Albert P. L. M. Goossens,[†] and Laurens D. A. Siebbeles[†]

Optoelectronic Materials, Faculty of Applied Sciences, Delft University of Technology, Julianalaan 136, 2628 BL Delft, The Netherlands, and School of Chemical and Biomolecular Engineering, Cornell University, 356 Olin Hall, New York

Received March 11, 2008; Revised Manuscript Received May 1, 2008

ABSTRACT

Efficient carrier multiplication has been reported for several semiconductor nanocrystals: PbSe, PbS, PbTe, CdSe, InAs, and Si. Some of these reports have been challenged by studies claiming that carrier multiplication does not occur in CdSe, CdTe, and InAs nanocrystals, thus raising legitimate doubts concerning the occurrence of carrier multiplication in the remaining materials. Here, conclusive evidence is given for its occurrence in PbSe nanocrystals using femtosecond transient photobleaching. In addition, it is shown that a correct determination of carrier-multiplication efficiency requires spectral integration over the photobleach feature. The carrier multiplication efficiency we obtain is significantly lower than what has been reported previously, and it remains an open question whether it is higher in nanocrystals than it is in bulk semiconductors.

Semiconductor nanocrystals (NCs) attract a great deal of attention for application as the light absorbing component in cheap and highly efficient solar cells. In particular, the exploitation of carrier multiplication (CM) in NCs has received a lot of interest, since this offers prospects for the development of solar cells with a maximum power conversion efficiency as high as 44%.[1,2] In the CM process, the excess energy of charge carriers produced by photons with energy greater than the band gap is utilized to produce additional charge carriers and is not lost in the form of heat.

A few years ago, Schaller et al. reported for the first time that carrier multiplication can be very efficient in semiconductor nanocrystals.[3] The observation of efficient CM is surprising since in bulk semiconductors it has been found to be inefficient at photon energies below ~5 times the band gap.[4–7] Since the first report on efficient CM in semiconductor nanocrystals,[3] this effect has become subject of intense research. A number of experimental studies reported the occurrence of CM in PbSe,[3,8–12] PbS,[8] PbTe,[13] CdSe,[12] InAs,[14,15] and Si[16] nanocrystals. The experimental determination of CM relies on the fast decay of multiexcitons as compared with a single exciton in an NC. This fast decay, assumed to be caused by Auger recombination, takes place on a time scale of tens of picoseconds, while the (radiative) decay of a single exciton takes tens of nanoseconds (CdSe) to microseconds (Si). The presence of multiexcitons can be monitored in pump−probe experiments by its effect on transient absorption (TA),[3,8] luminescence,[17,18] or terahertz conductivity.[14] In all instances, the observed signal changes with the fast decay of the multiexcitons. The difference between the signal just after pulsed photoexcitation and that at a longer time, when the multiexcitons have decayed, is a direct measure of the number of excitons generated per NC.

A strong controversy has arisen with respect to the occurrence of CM. Nair and Bawendi reported an elaborate analysis of transient photoluminescence measurements on CdSe and CdTe NCs and concluded that the CM efficiency is negligible,[17] in conflict with earlier reports on CdSe NCs.[12,18] Further, the earlier results of Pijpers et al. on CM in InAs NCs[14] have been withdrawn by the authors,[19] and an elaborate analysis showing that there is no detectable CM in this system was presented by Ben-Lulu et al.[20] The discussion focuses on the difficulty of comparing the measured transients at different photon energies of the exciting laser pulse. The absorption cross section of NCs strongly depends on the photon energy, as shown in Figure 1. For high optical densities the spatial intensity profile (the Lambert−Beer profile) of the pump beam varies strongly across the cuvette containing the solution of NCs. Even though the cuvette-

* Corresponding author. E-mail: j.m.schins@tudelft.nl (J.M.S.) and a.j.houtepen@tudelft.nl (A.J.H.).
[†] Delft University of Technology.
[‡] Cornell University.

10.1021/nl0807225 CCC: $40.75
Published on Web 05/20/2008

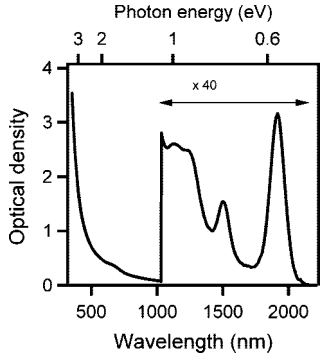

Figure 1. Optical absorption spectrum of 6.8 nm PbSe NCs in tetrachloroethylene. For wavelengths above 1000 nm, the spectrum has been multiplied by 40.

averaged number of absorbed photons per NC is small, at the entrance of the cuvette, multiphoton absorption can still occur, leading to a probe signal identical to that observed in the case of CM.

Although the papers by Nair and Bawendi[17] and by Ben-Lulu et al.[20] formally only show that CM was not observed in their respective NC systems, they cast serious doubt on the experimental reports of CM in all nanocrystal materials. The present work aims at dispelling these legitimate doubts by establishing conclusively the occurrence of CM in PbSe NCs. To arrive at a conclusive and correct determination of CM, three issues are addressed. First, it is shown that it is possible to reach conditions under which sequential multiphoton absorption can be discarded. This condition is met at very low excitation power, when the measured number of excitons per excited NC becomes independent of pump fluence. Second, it is demonstrated that the measured decays of the transient photobleaching signals are not due to trap states for charges but can only be due to CM. This establishes qualitatively the occurrence of CM in PbSe NCs. The third issue concerns the quantitative determination of the CM efficiency from spectral integration: it is shown that the correct CM efficiency can not be determined from the transient signal measured at a single probe wavelength due to excitation-induced shifts in the absorption spectrum.

Dispersions of oleic acid-capped PbSe NCs were prepared following the recipe of Talapin and Murray.[21] Lead(II) oleate was prepared from 2.16 g lead(II) acetate trihydrate and 7.3 mL oleic acid by heating a mixture of these chemicals in 40 mL squalane under vacuum. A 14.2 mL sample of the resulting Pb-oleate stock solution was heated to 150 °C at which point 5.4 mL of 1.0 M selenium in trioctyl phosphine was injected employing 1 bar overpressure in a Schlenk line. The NCs were allowed to grow for 5 min resulting in monodisperse, quasi-spherical NCs with diameters of 6.8 nm, determined from the energy of the first exciton absorption (0.65 eV) and the calibration provided in ref 22. The absorption spectrum of the NCs is shown in Figure 1. The full width at half-maximum of the first absorption feature is only 42 meV, showing that these NCs are very monodisperse. The NCs were precipitated twice by the addition of a butanol−methanol mixture (2:1 v/v) and collected by centrifugation. Finally, the NCs were dispersed in tetrachloroethylene for the measurements. The solution is carefully kept free from oxygen and water contamination, both during its preparation and during the measurement.

The NCs were excited and monitored by pump and probe pulses from a chirped-pulse amplified laser system (Mira-Legend USP, Coherent Inc.), which runs at 1 kHz and delivers pulses of 60 fs, 2.2 mJ, at a 795 nm wavelength. Tunable infrared and visible pulses (<100 fs) were generated by optical parametric amplification seeded by white light (Topas-800-fs and Opera, Coherent Inc.) and from frequency doubling. Pump and probe beams overlapped under a small angle (3°) in a cuvette of 10 mm path length and were imaged onto InGaAs pin-photodiodes (Hamamatsu G5853−23, G8605−23). The optical density of the sample was OD = 0.075 at the first exciton peak (cf. Figure 1). Both pump and probe beams were not focused. The pump beam diameter was 8 mm; the probe beam diameter was 0.5 mm. The two beams were spatially separated downstream from the sample. The orthogonal polarization of the beams allowed further separation by means of a polarizer.

Exclusion of Multiphoton Absorption. The most important complicating factor in the determination of carrier multiplication is the occurrence of sequential multiphoton absorption. This creates in a trivial way multiexcitons, which have a signature that is identical to that of multiexcitons created by CM. The first issue that is addressed here concerns the conditions under which sequential multiphoton absorption can be ruled out as a source for multiexciton generation.

The number of photons that is absorbed by the NCs depends on the product $J\sigma$ of the photon flux J and the NC absorption cross section σ. Since the photon flux decreases exponentially as the beam traverses the sample, the average number of photons absorbed per nanocrystal is given by[23]

$$\begin{aligned} N_{abs} &= \frac{1}{L}\int_0^L \mathrm{d}z\, J(z)\sigma \\ &= \frac{1}{L}\int_0^L \mathrm{d}z\, J(0)\, \mathrm{e}^{-\alpha z}\sigma \\ &= J(0)\sigma\frac{1-\mathrm{e}^{-\alpha L}}{\alpha L} \\ &= J(0)\frac{1-\mathrm{e}^{-\alpha L}}{cL} \end{aligned} \tag{1}$$

Here, L is the length of the cuvette, $J(0)$ is the photon flux at the cuvette's entrance, α is the absorption coefficient at the pump wavelength, and c is the concentration of nanocrystals in the solution. The factor αL, related to the optical density OD as $\alpha L = \mathrm{OD}\ \ln 10$, follows directly from the absorption spectrum in Figure 1.

The probability for a NC to absorb N photons, for a given average number of absorbed photons $J\sigma$, is described by the Poisson distribution:

$$P_N = \frac{(J\sigma)^N}{N!}\,\mathrm{e}^{-J\sigma} \tag{2}$$

It follows that in the limit of vanishingly small fluence only single excitons are created but that at higher fluence the probability of multiphoton absorption increases rapidly. Note that the distribution in eq 2 varies over the depth in the cuvette, since the fluence J decreases according to the

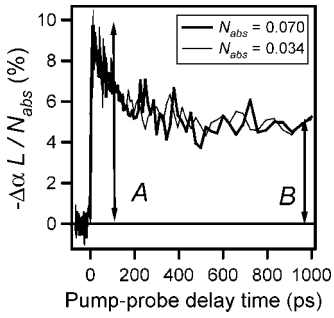

Figure 2. Low-fluence TA traces corresponding to different values of the average number of absorbed photons per nanocrystal (see inset). Pump photon energy, 3.1 eV; probe photon energy, 0.65 eV (corresponding to the first exciton peak). The vertical axis displays the change in absorption normalized by N_{abs}, the average number of absorbed photons per NC.

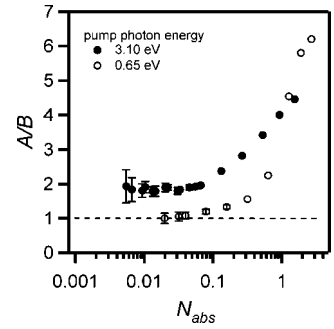

Figure 3. Differential absorption ratio A/B versus the average number of absorbed photons per NC. The low-fluence convergence (the "plateau") of the differential absorption ratio to a value higher than unity is a signature of carrier multiplication. CM occurs for 3.1 eV pump photon energy (4.8 times the band gap) and is absent for 0.65 eV pump photon energy (1.0 times the band gap). The error bars represent the shot noise averaged over 8000 shots.

Lambert−Beer law. The quantitative determination of the cross section σ, needed for the calculation of the number of absorbed photons, is discussed below (see Figure 6).

In Figure 2, two TA traces are shown[24] for different values of the average number of absorbed photons per NC, N_{abs}. The PbSe nanocrystals were pumped at 3.1 eV (4.8 times the band gap energy) and probed at 0.65 eV (the energy of the $1S_h1S_e$ exciton absorption maximum). The traces show an initial steep rise (about 3 ps, the time needed for the hot carriers to relax to the band edge[25]), followed by an exponential decay on a time scale of ∼100 ps, which is usually assigned to Auger recombination of two band-edge excitons to a single hot exciton.[3] The surviving species is a single $1S_h1S_e$ band-edge exciton, with a lifetime of about 800 ns,[26] which largely exceeds our 1 ns time window. Since the induced photobleach is linear with the number of excitons in the nanocrystal,[3] the ratio of differential absorption at small and large values of the pump−probe time delay τ, $\Delta\alpha$ (τ = 3 ps)/$\Delta\alpha$ (τ = 1 ps), labeled A/B from here on (cf. Figure 2), is a measure of the initially generated number of excitons per excited NC, the exciton multiplicity N_x (not to be confused with N_{abs}, the average number of excitons per NC). The multiplicity N_x may be induced by CM or by multiphoton absorption. Both multiphoton absorption and CM may lead to the creation of multiexcitons above $N_x = 2$. Since the TA signals in Figure 2 are normalized to N_{abs}, the traces should overlap in the low fluence limit. For the traces shown, this is indeed the case: a change in fluence of a factor 2 does not affect the traces. This is a first clear signature of the absence of multiphoton absorption.

The shot noise of the traces increases for decreasing fluence, as fixed accumulation times have been used (2000 laser shots per data point). To measure the exciton multiplicity reliably at even lower laser fluence than that used in Figure 2, we restricted the TA measurements to only two delay times, τ = 3 ps and τ = 1 ns, while averaging the signals over many laser shots. The results of these measurements are shown in Figure 3.

The pump photon energy was 3.1 or 0.65 eV, while the probe photon energy was equal to 0.65 eV. Every data point in the figure represents 5 measurements of each 8000 laser shots. The error bars indicate the standard deviation of those five measurements. In the case of pure shot noise (for the lowest fluences shot noise indeed dominates over all other noise sources), the error bars scale with the inverse square root of the number of laser shots averaged. The data points were measured over nearly 3 orders of magnitude of fluence.[27] At low fluence, there is a plateau extending over a decade of N_{abs}, with $A/B \approx 1.8$ for 3.1 eV, while at a pump photon energy of 0.65 eV, the ratio A/B clearly converges to 1.0. The ratio A/B is independent of the fluence below $N_{abs} = 0.05$, and it is concluded that multiphoton absorption does not contribute to its value. To our knowledge, this is the first time that such a fluence-independent regime is observed. It was recognized previously that such a regime should occur, but the corresponding experiments were not performed at sufficiently low fluence to exhibit a clear plateau.[16,28]

Exclusion of Trapping Effects. The second issue addressed in this Communication concerns the demonstration that the decay of the measured TA signals during time are not due to electron or hole trapping at defect sites but can only be due to CM. A trapping mechanism that leads to a photobleach that is large after ∼3 ps and subsequently decreases could possibly produce the TA traces shown in Figure 2. Figure 4 shows the difference between CM and such a trapping mechanism, which would involve rapid trapping of the initially highly excited electron (or hole). As a result, the photobleach after ∼3 ps could be caused by the surviving hole (electron) only. Recombination of the trapped electron with the hole would then lead to the decay of the TA signal.

A trapping process able to account for the TA traces in Figure 2 must satisfy several conditions. First, the energy of the trapping state must exhibit a threshold in pump photon energy, below which the effect of trapping is absent. Second, the trapping rate must be comparable to or faster than the cooling rate of the hot carriers (∼3 ps). Third, the relaxation of the trapped state to the ground state should occur with a decay time of ∼100 ps. Fourth, relaxation of the trapped electron (hole) should occur by recombination with the hole (electron), since decay of the trapped state to the $1S_h1S_e$ exciton state would produce an increasing TA signal, in

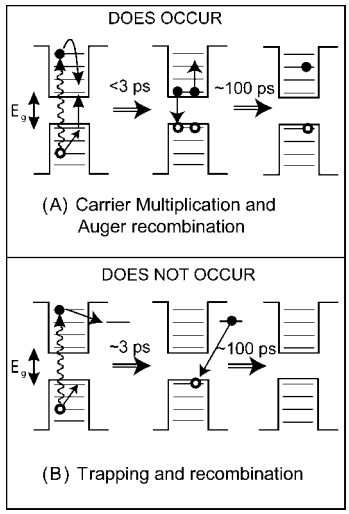

Figure 4. (A) Schematic representation of carrier multiplication followed by Auger recombination and (B) the trapping mechanism discussed in the text. The trapping mechanism for the hole is not represented in the figure but is similar to that shown in the lower panel for the electron. Both scheme A and B result in a photobleach that decays with time.

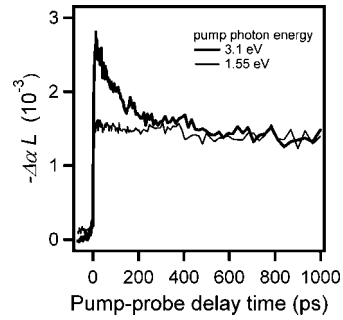

Figure 5. Comparison of the absolute value of the photobleach after photoexcitation below (1.55 eV) and above (3.1 eV) the energy threshold for CM. The fluences have been chosen such that an equal number of pump photons is absorbed in both cases. At long times, the TA traces converge to the same value of differential absorption $\Delta\alpha L$, implying that the final yield of excitons is identical in both cases. The baselines have been carefully checked; the trace pumped at 1.55 eV starts out at $-\Delta\alpha L = 10^{-4}$ because of a prepulse originating from the laser amplifier.

disagreement with the measured decay in Figure 2. While it would be quite coincidental for a trapping mechanism to have all of the above properties, it cannot be excluded a priori.

Trapping can be distinguished from CM in an experiment that compares super- with subthreshold pumping. This must be done for low fluence and for an equal amount of pump photons absorbed in the sample. In that case, the absolute signals at long delay times are a direct measure of the branching ratio of CM versus trapping. Under these circumstances, three essential conditions are fulfilled: (i) long delay times ensure that eventual CM effects do not contribute to the signal, since the multiexcitons have decayed to single excitons; (ii) low fluence ensures that any nanocrystal absorbs at most single pump photons; and (iii) equal amounts of absorbed pump photons ensure the excitation of equal numbers of nanocrystals.

The above conditions were satisfied for the two traces shown in Figure 5. Subthreshold excitation was realized at 1.55 eV. Indeed, the trace pumped at 1.55 eV has no 100 ps decay component. This proves at once the absence of CM, of trapping (in the sense of Figure 4B), and of multiphoton absorption. All absorbed photons are converted into band-edge excitons, thus contributing equally to the long-time TA signal. Superthreshold excitation was realized at 3.1 eV pump photon energy. The TA trace exhibits a clear 100 ps decay component. Yet the signal at 1 ns delay time is equal in magnitude to the TA signal of the subthreshold excited trace. This implies that at 1 ns delay there is an equal number of excitons for both pump photon energies. Since in the subthreshold case every single pump photon was converted into an exciton, this must also be the case in the superthreshold case. From which it follows that there can be no trapping in the sense of Figure 4B in the superthreshold case. Consequently, the excess TA signal at short times must be due to CM.

The pump photon energy of 3.1 eV (400 nm wavelength) corresponds to 4.8 times the band gap energy, and 1.55 eV (800 nm wavelength) corresponds to 2.4 times the band gap energy. The pump fluences J_{400} and J_{800} were chosen such that the average number of photons N_{abs} absorbed throughout the cuvette is equal for both pump wavelengths: $J_{400}(0)(1 - e^{-\alpha_{400}L}) = J_{800}(0)(1 - e^{-\alpha_{800}L})$, as implied by eq 1. The traces in Figure 5 were measured at $J_{800}(0) = 3.8 \times 10^{13}$ photons/cm^2 and at $J_{400}(0) = 0.6 \times 10^{13}$ photons/cm^2, respectively.

The value of $\Delta\alpha$L at long time delay ($\tau = 1$ ns) was used to determine the cross section for photon absorption at the probe wavelength. Figure 6 shows the measured values of $\Delta\alpha L$ at 1 ns delay time as a function of pump fluence. The values of $\Delta\alpha L$ are presented as a function of the quantity $J(0)(1 - e^{-\alpha L})$, which scales linearly with the cuvette-averaged number of absorbed photons per nanocrystal, N_{abs} (see eq 1). The slope of the line in Figure 6 is proportional to the cross section at the probe wavelength, σ_{1920}. Since the lowest quantum confined states in PbSe are 8-fold degenerate, the change in the relative absorption coefficient of the $1S_h1S_e$ transition amounts to 1/4 per exciton (i.e., per absorbed photon):

$$\frac{-\Delta\alpha_{1920}}{\alpha_{1920}} = \frac{1}{4}N_{abs} \quad (3)$$

where N_{abs} is given by eq 1, and $\Delta\alpha_{1920}$ represents the change in absorption coefficient at $\lambda_{probe} = 1920$ nm for the single exciton state. In the low fluence limit (such that no multiphoton absorption occurs), the differential absorption measured at a delay of 1 ns relates linearly to the cross section:

$$-\Delta\alpha(1\text{ ns})L = \frac{1}{4}N_{abs}\alpha_{1920}L = \frac{\sigma_{1920}}{4}J(0)(1 - e^{-\alpha_{pump}L}) \quad (4)$$

Equations 3 and 4 do not take into account the fact that the $1S_h1S_e$ transition shifts because of excitonic population. As will be shown below, this exciton-induced spectral shift can be quantified rigorously. With this effect taken into account $\sigma_{1920} = 14$ Å^2 is obtained from the data shown in

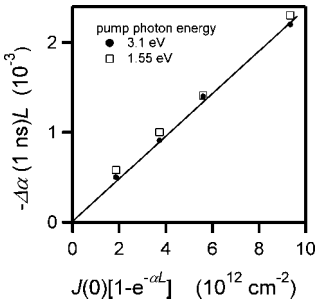

Figure 6. Differential absorption ratio ΔαL at 1 ns delay time as a function of $J(0)(1 - e^{-\alpha L})$ for both superthreshold (solid circles, 3.1 eV photon energy) and subthreshold (open squares, 1.55 eV) excitation.

Figure 6. Our value exceeds the value obtained by Luther et al.[28] by about 40% but is in excellent agreement with the extensive study of Moreels et al.[29] For PbSe NCs of 6.8 nm diameter, Moreels et al. find $\sigma_{400} = 340$ Å^2, where we deduce, using the absorption spectrum of Figure 1, $\sigma_{400} = 330$ Å^2. This value, together with $\sigma_{1920} = 14$ Å^2, was used to determine N_{abs} in Figures 2 and 3.

Spectral Integration. The third issue addressed in this Communication concerns the correct determination of the CM efficiency from TA transients such as those shown in Figure 2. The excitonic transitions in NCs are sensitive to the presence of spectator charges in the environment. The addition of excitons[30] or charges[31] typically lowers the energy of these transitions. The magnitude of the corresponding red shift depends on the number of excitons (or charges) added to the NC and changes in time as the exciton population changes in time (e.g., because of CM or multiphoton absorption). The time-dependent spectral shift induces an error in the CM efficiency determined from the ratio *A*/*B* at a single probe wavelength.

This effect is illustrated in Figure 7, which shows the photobleach at different delay times and as a function of probe wavelength (upper pane). At 3 ps delay (open circles), the nanocrystals contain on average slightly less than 2 excitons, which induce a larger shift on the $1S_h1S_e$ transition than at 1 ns delay (open squares), when all excited nanocrystals contain only a single exciton.[32]

The spectral shifts can be dealt with in a straightforward manner. For a correct assessment of the CM efficiency η_{CM}, it suffices to integrate the TA signals spectrally,

$$\eta_{CM} = \lim_{J\to 0} \frac{\int dE \Delta\alpha(\tau = 3\text{ ps})}{\int dE \Delta\alpha(\tau = 1\text{ ns})} \qquad (5)$$

where the probe energy E ranges over the absorption feature. For the 6.8 nm sized PbSe nanocrystals studied in the present work, the difference between the differential absorption ratio *A*/*B* at the maximum of the absorption feature and the carrier multiplication efficiency η_{CM} turns out to be quite small: $A/B = 1.8$ versus $\eta_{CM} = 1.7$. However, this correction becomes important for high values of the exciton multiplicity. This is for example the case for the 0.65 eV pump data shown in Figure 3. At the highest fluence ($N_{abs} \approx 3$) for 0.65 eV pump photon energy, the differential absorption ratio is $A/B = 6.0$,

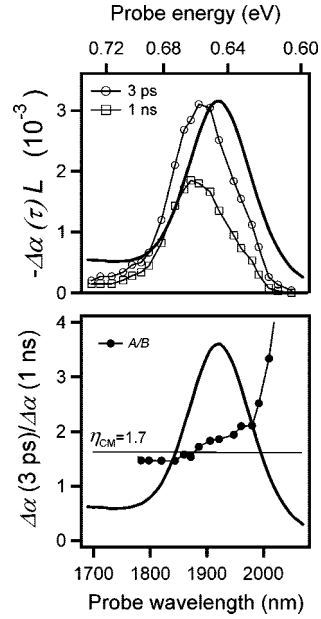

Figure 7. Differential absorption $\Delta\alpha L$ as a function of probe wavelength for short ($\tau = 3$ ps, open circles) and long ($\tau = 1$ ns, open squares) pump−probe delays measured at low fluence and 3.1 eV pump photon energy (upper pane). The ground-state absorption spectrum (continuous black line) has been scaled arbitrarily and is shown in both panes for reference. The solid circles represent the values of the differential absorption ratio *A*/*B* (lower pane). While *A*/*B* is roughly constant towards the blue of the absorption maximum, it diverges toward the red. The chromatism of *A*/*B* becomes worse when multiple excitons are involved, illustrating the necessity of spectral integration for a correct determination of CM efficiency ($\eta_{CM} = 1.7$, horizontal line).

while the chromatic integration procedure results in an average number of excitons per excited NC of $N_x = 3.9$. The latter value is in agreement with the 8-fold degeneracy of the 1S levels in PbSe, since for pumping at 0.65 eV (at resonance with the first exciton transition) the population of excitons should converge to half the degeneracy of the 1S levels. In that case, the sample becomes transparent for the probe beam, because the rate of stimulated emission equals the rate of absorption. In general, one should be careful with interpreting *A*/*B* as the ratio of exciton populations at short and long time; that ratio depends on probe wavelength, as is shown in Figure 7 (black triangles, plotted against the vertical axis at the right). Specifically, probe wavelengths toward the red large errors result upon estimating the CM efficiency from *A*/*B*.

From the above analysis, it is clear that CM does occur in PbSe nanocrystals. This conclusion differs from recent claims that CM is absent in CdSe, CdTe,[17] and InAs[20] NCs. However, the highest values of the excitation energy used in those papers were 3.1[17] and 3.7[20] times the band gap. The experiments presented here were performed at 4.8 times the band gap, which makes a direct comparison of the CM efficiency difficult.

The CM efficiency of $\eta_{CM} = 1.7$ obtained at a photon energy of 4.8 times the band gap is significantly lower than that previously reported by Schaller et al.[9] ($\eta_{CM} > 3$). The comparison is straightforward, because the band gap of the particles investigated in ref 9 was almost identical to the

band gap of the NCs studied here (0.64 and 0.65 eV, respectively). Consequently, differences in confinement-enhanced Coulomb interaction cannot explain the discrepancy. Rather, the three issues discussed in the present Communication (multiphoton absorption, trapping, and spectral integration) may have affected the determination of the high CM efficiencies in ref 9.

The CM efficiency observed in the present work is only slightly higher than that reported for bulk Si[5,7] and Ge.[7] In Ge, a CM efficiency of 1.7 was observed for excitation near 6 times the band gap (compared to 4.8 times for the PbSe NCs investigated here). To the knowledge of the authors, the only available report on CM in bulk Pb-chalcogenide semiconductors is that by Smith and Dutton[4] from 50 years ago. They observed CM in PbS with a threshold of $\sim$5 E_g and an efficiency of 1.7 around $\sim$9 E_g. However, it is not clear how to relate these measurements to the picosecond-resolved quantities measured here. As a matter of fact, in all bulk studies mentioned above, the determination of CM was done by measurement of the photocurrent in a diode. Such a measurement presents a lower limit of the instantaneous CM efficiency, since the carrier collection efficiency may be smaller than unity. Therefore, an important question remains whether CM is truly enhanced in NCs. Currently, work is in progress which aims at providing a fair comparison between bulk and nanocrystal PbSe with respect to their CM capacity.

In conclusion, the energy- and fluence-dependent analysis of transient photobleaching presented in this Communication provides compelling support for the occurrence of carrier multiplication in PbSe nanocrystals, while at the same time questioning the role of quantum confinement.

Acknowledgment. This work is part of the Joint Solar Programme (JSP) of the Stichting voor Fundamenteel Onderzoek der Materie (FOM). J.S.P. is cofinanced by "Gebied Chemische Wetenschappen" of the Dutch Organisation for Scientific Research (NWO) and by Stichting Shell Research. We furthermore acknowledge the 3TU Centre for Sustainable Energy Technologies (Federation of the three Universities of Technology) and the Division of Chemical Sciences of NWO for the VICI Award No. 700.53.443.

References

(1) Nozik, A. J. *Physica E* **2002**, *14*, 115–120.
(2) Hanna, M. C.; Nozik, A. J. *J. Appl. Phys.* **2006**, *100*, 074510.
(3) Schaller, R. D.; Klimov, V. I. *Phys. Rev. Lett.* **2004**, *92*, 186601.
(4) Smith, A.; Dutton, D. *J. Opt. Soc. Am.* **1958**, *48*, 1007.
(5) Wolf, M.; Brendel, R.; Werner, J. H.; Queisser, H. J. *J. Appl. Phys.* **1998**, *83*, 4213–4221.
(6) Guyot-Sionnest, P. *Nat. Mater.* **2005**, *4*, 653–654.
(7) Christensen, O., Quantum efficiency of the internal photoelectric effect in silicon and germanium. In *AIP* 1976; Vol. 47, pp 689−695.
(8) Ellingson, R. J.; Beard, M. C.; Johnson, J. C.; Yu, P.; Micic, O. I.; Nozik, A. J.; Shabaev, A.; Efros, A. L. *Nano Lett.* **2005**, *5*, 865–871.
(9) Schaller, R. D.; Sykora, M.; Pietryga, J. M.; Klimov, V. I. *Nano Lett.* **2006**, *6*, 424–429.
(10) Schaller, R. D.; Klimov, V. I. *Phys. Rev. Lett.* **2006**, *96*, 097402.
(11) Schaller, R. D.; Agranovich, V. M.; Klimov, V. I. *Nat. Phys.* **2005**, *1*, 189–194.
(12) Schaller, R. D.; Petruska, M. A.; Klimov, V. I. *Appl. Phys. Lett.* **2005**, *87*, 253102.
(13) Murphy, J. E.; Beard, M. C.; Norman, A. G.; Ahrenkiel, S. P.; Johnson, J. C.; Yu, P. R.; Micic, O. I.; Ellingson, R. J.; Nozik, A. J. *J. Am. Chem. Soc.* **2006**, *128*, 3241–3247.
(14) Pijpers, J. J. H.; Hendry, E.; Milder, M. T. W.; Fanciulli, R.; Savolainen, J.; Herek, J. L.; Vanmaekelbergh, D.; Ruhman, S.; Mocatta, D.; Oron, D.; Aharoni, A.; Banin, U.; Bonn, M. *J. Phys. Chem. C* **2007**, *111*, 4146–4152.
(15) Schaller, R. D.; Pietryga, J. M.; Klimov, V. I. *Nano Lett.* **2007**, *7*, 3469–3476.
(16) Beard, M. C.; Knutsen, K. P.; Yu, P. R.; Luther, J. M.; Song, Q.; Metzger, W. K.; Ellingson, R. J.; Nozik, A. J. *Nano Lett.* **2007**, *7*, 2506–2512.
(17) NairG.; Bawendi, M. G. *Phys. Rev. B* **2007**, *76*, 081304(R).
(18) Schaller, R. D.; Sykora, M.; Jeong, S.; Klimov, V. I. *J. Phys. Chem. B* **2006**, *110*, 25332–25338.
(19) Pijpers, J. H. H.; HendryE.; Milder, M. T. W.; Fanciulli, R.; Savolainen, J.; Herek, J. L.; Vanmaekelbergh, D.; Ruhman, S.; Mocatta, D.; Oron, D.; A., A.; Banin, U.; Bonn, M. *J. Phys. Chem. C* **2008**, *112*, 4783–4784.
(20) Ben-Lulu, M.; Mocatta, D.; Bonn, M.; Banin, U.; Ruhman, S. *Nano Lett.* **2008**, *8*, 1207.
(21) Talapin, D. V.; Murray, C. B. *Science* **2005**, *310*, 86–89.
(22) Koole, R.; Allan, G.; Delerue, C.; Meijerink, A.; Vanmaekelbergh, D.; Houtepen, A. J. *Small* **2008**, *4*, 127–133.
(23) The integral of eq 1 really describes the number of photon interactions with the electromagnetic field, rather than the number of absorbed photons. However, discrepancies between the number of photon interactions (absorption or emission) and the number of absorbed photons are negligible, except for the highest fluences in Figure 3.
(24) The values for $\Delta\alpha L$ were obtained from the measured probe transmissions T_{on} (pump on) and T_{off} (pump off) assuming the Lambert−Beer law $T_{on} = T_{off}\, e^{-\Delta\alpha L}$, with $\Delta\alpha \equiv \alpha_{on} - \alpha_{off}$. This procedure is justified since (i) the reflection of the pump beam off the exit interface is negligible, as is (ii) the pump-induced reflection of the probe beam off the entrance interface.
(25) Schaller, R. D.; Pietryga, J. M.; Goupalov, S. V.; Petruska, M. A.; Ivanov, S. A.; Klimov, V. I. *Phys. Rev. Lett.* **2005**, *95*, 196401.
(26) Wehrenberg, B. L.; Wang, C. J.; Guyot-Sionnest, P. *J. Phys. Chem. B* **2002**, *106*, 10634–10640.
(27) The inflection at high pump fluence for the 0.65 eV data is not an artifact and is commented on in the context of eq 5. The dependence of exciton multiplicity on fluence is an interesting subject by itself and will be dealt with in a forthcoming paper. The crossing of the two curves in Figure 3 is due to multiplicity-dependent spectral shifts of the first exciton level, as explained in detail in the section on spectral integration.
(28) Luther, J. M.; Beard, M. C.; Song, Q.; Law, M.; Ellingson, R. J.; Nozik, A. J. *Nano Lett.* **2007**, *7*, 1779–1784.
(29) Moreels, L.; Lambert, K.; De Muynck, D.; Vanhaecke, F.; Poelman, D.; Martins, J. C.; Allan, G.; Hens, Z. *Chem. Mater.* **2007**, *19*, 6101–6106.
(30) Klimov, V. I. *Annu. Rev. Phys. Chem.* **2007**, *58*, 635–673.
(31) Houtepen, A. J.; Vanmaekelbergh, D. *J. Phys. Chem. B* **2005**, *109*, 19634–19642.
(32) Exciton populations influence not only the shifts but also the magnitude of the TA signals. Consequently, the peak separations of the TA signals with respect to the ground-state absorption feature may not be identified with the $1S_h1S_e$ shifts. This is illustrated in Figure 7 (upper pane): the TA signal at 3 ps peaks in between the ground state absorption and the TA signal at 1 ns.

NL0807225